Determination of trace bismuth by under-potential deposition–stripping voltammetry at mesoporous platinum microelectrodes: Application to pharmaceutical products

ARTICLE *in* JOURNAL OF SOLID STATE ELECTROCHEMISTRY · JUNE 2013

Impact Factor: 2.45 · DOI: 10.1007/s10008-013-2084-5

2 AUTHORS:

Dario Battistel
Università Ca' Foscari Venezia
25 PUBLICATIONS **208** CITATIONS
SEE PROFILE

S. Daniele
Università Ca' Foscari Venezia
138 PUBLICATIONS **2,063** CITATIONS
SEE PROFILE

J Solid State Electrochem (2013) 17:1509–1516
DOI 10.1007/s10008-013-2084-5

ORIGINAL PAPER

Determination of trace bismuth by under-potential deposition-stripping voltammetry at mesoporous platinum microelectrodes: application to pharmaceutical products

Dario Battistel · Salvatore Daniele

Received: 21 January 2013 / Revised: 29 March 2013 / Accepted: 31 March 2013 / Published online: 10 April 2013

Abstract A methodology for the determination of bismuth, based on under-potential deposition-stripping voltammetry (UPD-SV), was investigated. It makes use of mesoporous platinum microelectrodes (Pt-MEs) prepared by a liquid crystal templating technique. The mesoporous microelectrodes, which are characterised by a very high surface area, allowed the accumulation of relatively large amounts of bismuth at under-potential without saturation of the electrode surface. Calibration plots for quantification of bismuth at micromolar levels were constructed by using the charge involved in either the anodic or cathodic peak recoded by cyclic voltammetry that ensued the accumulation of bismuth at the electrode surface. During the anodic scan, the oxidation of metallic bismuth occurred; the cathodic scan involved irreversibly adsorbed bismuth species, which are retained on to the electrode surface. The reproducibility of the proposed UPD-SV procedure (which was within 5 %) was assured by the application to the Pt-MEs of a suitable potential waveform, properly designed to avoid memory effect due to the irreversibly deposited bismuth. The latter phenomenon along with UPD allowed to overcome interference due to copper, which is normally observed when quantification of bismuth is performed by anodic stripping voltammetry at solid electrodes involving bulk metal deposits. The usefulness of the proposed method for the determination of bismuth in real samples was demonstrated by the analysis of a tablet of a pharmaceutical preparation, which is used for curing ulcers.

Keywords Bismuth detection · Under-potential deposition · Mesoporous platinum · Microelectrodes · Pharmaceutical products

Introduction

Stripping voltammetry (SV) is one of the most sensitive and multi-element analysis technique for the detection of a large variety of trace metals at low detection limits [1]. Its remarkable sensitivity is achieved through a pre-concentration step, in which the investigated species is accumulated into or onto working electrodes [2]. This step is followed by the stripping step resulting in a voltammetric signal proportional to the concentration of the analyte in the sample [2]. Mercury has been the electrode material of choice, because of its well-known properties, such as its very smooth surface area and high hydrogen overvoltage, which makes it ideal for stripping measurements of metal ions over the negative potential region in aqueous media. However, concerns on mercury toxicity have recently led to a growing interest in the development of alternative electrode systems and methods with performance approaching that based on mercury [3, 4]. To this purpose, solid electrodes (carbon and carbon glass, gold, iridium, platinum and silver), various types of solid amalgams and more new exotic materials (for instance, doped diamond) have been considered [3, 5]. As regards to the detection of metal ions by anodic stripping voltammetry (ASV), solid electrodes suffer from interference due to the formation of inter-metallic compounds and multiple peaks for the same element (due to the formation of mono- or multi-layers or bulk metal deposits), which make the analytical signals difficult to interpret [5]. To overcome these problems, several strategies, encompassing different voltammetric waveforms [6], electrode surface coated with thin

For the special issue dedicated to Prof. Brainina.

D. Battistel · S. Daniele (✉)
Dipartimento di Scienze Molecolari e Nanosistemi, Università Cà Foscari Venezia, Calle Larga S. Marta, 2137,
30123 Venice, Italy
e-mail: sig@unive.it

films of bismuth [4, 7] or antimony [8], and under-potential deposition (UPD) [9] have been considered.

UPD is typical for solid electrodes and describes the formation of sub-mono-layers up to a mono-layer of material at potentials anodic the Nernst potential at which bulk deposition of the metal occurs [10]. UPD, in conjunction with ASV, offers several advantages over the use of bulk metal deposition [9]. At under-potential and under the conditions of trace elements analysis, the deposit covers a low portion of the working electrode surface, and because of the limited amount of material deposited, mutual interference between metals deposited is minimal, while the pre-concentration step is often short. In addition, the structure of the electrode remains essentially unchanged, which results in a good analytical repeatability of the SV responses. As UPD is very sensitive to the nature of the electrode substrate, the choice of the working electrode is very important. Silver, gold and carbon electrodes of conventional dimensions (i.e., characteristic dimension in the millimetre range) have been used for UPD-ASV measurements of Cu, Hg, Pb, and Cd [9]. Platinum has been widely investigated as a substrate for UPD of numerous metals [10–12]. However, it has rarely been used for UPD-ASV measurements. Only recently, electrodes modified by a thin film of mesoporous platinum have been employed for analytical quantification of metal ions by UPD-ASV [13, 14]. In particular, mesoporous rotating disk electrodes [14] and mesoporous microelectrodes [13], fabricated by a liquid crystal templating technique [15], have been used for trace analysis of Ag^{+}, Pb^{2+} and Cu^{2+} ions at micromolar levels. In the UPD-ASV context, the mesoporous electrodes, which are characterised by a very large surface area and long-range nanoscale order [15], have displayed useful analytical performance and advantages over smooth electrodes. In particular, larger amounts of metal UPD can be accumulated before maximum saturation of the electrode surface occurs, thus enhancing sensitivity. Moreover, because metal UPD involves mainly the internal pores of the mesoporous structure, interference arising from high molecular organic compounds, such as Tween 20 and Triton X-100, is minimal [13, 14].

In view of expanding the use of mesoporous microelectrodes for UPD-SV to other metal ions and verify potential applications of UPD-SV for trace metal analysis in real world samples, in this paper, for the first time, we report on the use of mesoporous platinum microelectrodes for the determination of Bi^{3+} ions.

Bismuth is a rare element, used in several fields, as for instance in metallurgy, as an additive of low melting-point alloys and free-machining steel; in cosmetic industry, for the preparation of creams and hair dyes; in pharmaceutical preparations, as antiulcer, antibacterial, anti-HIV and radiotherapeutic agents [16]. Thus, because of its widespread use, there is a need for accurate, inexpensive and rapid methods of quantification of bismuth in several matrices and for industrial quality control. The potential of the UPD-SV at mesoporous microelectrodes for practical applications in real samples is also demonstrated here in the detection of bismuth in a pharmaceutical preparation.

Experimental

Chemicals, reagents and sample analysed

All chemicals employed were of analytical reagent grade. Hexachloroplatinic acid (HCPA), sulphuric and nitric acid, ethylendiamine-tetraacetic acid disodium salt (EDTA) were from Carlo Erba; potassium chloride, the surfactant octaethylene glycol monohexadecyl ether ($C_{16}EO_8$), $Bi(NO_3)_3$ standard solution (1,005 μg/L+5 wt % HNO_3) and hexaammine ruthenium(III) chloride were purchased from Aldrich. Tablets of the anti-ulcer De-Nol® were purchased from the local pharmacy. All chemicals were used as received, and all aqueous solutions were prepared with deionised water purified via a Milli-Q unit (Millipore system). Unless otherwise stated, all measurements were performed in solutions purged with pure nitrogen (99.99 % from SIAD) and at room temperature (21±1 °C).

Liquid crystalline plating mixture

The liquid crystalline plating mixture was composed of 42 % (w/w) $C_{16}EO_8$, 29 % (w/w) HCPA and 29 % (w/w) Milli-Q water [15, 17–22]. This mixture allowed producing a stable hexagonal phase through efficient mixing of the components, employing a vortex mixer, while subjecting the mixture to three heating–cooling cycles from 20 to 80 °C [17–22]. Prior to further use, the liquid crystalline phase was allowed to equilibrate for 24 h at room temperature.

Electrodes and instrumentation

The smooth disk microelectrodes were prepared by sealing 12.5 μm radius platinum wires into glass capillaries. Pt-MEs were prepared by electrodeposition of platinum films onto the platinum disk microelectrode from the liquid crystalline plating mixture [13, 15, 17–22]. The electrodeposition was carried out at constant potential at about −0.6 V against a platinum spiral used as pseudo reference electrode. After deposition, the mesoporous electrodes were allowed to soak in Milli-Q water for 12–24 h to remove the surfactant. The electrodes thus prepared were stored in a 0.1 M H_2SO_4 solution up to their use.

The geometric and real surface areas of both smooth and mesoporous platinum microelectrodes were determined by, respectively, steady state voltammetry in 1 mM $Ru(NH_3)_6Cl_3$ solution containing 0.1 M KCl, and in 0.5 M sulphuric acid by

analysis of hydrogen UPD, as reported in detail elsewhere [17–22]. The ratio between the real and the geometric surface area of the electrode provided the roughness factor (*RF*). The Pt-MEs employed here were characterised by *RF* values, which varied in the range 140–300.

All electrochemical experiments were carried out in a two-electrode cell maintained in a Faraday cage made of sheets of aluminium to minimise external interference. Cyclic voltammetry (CV) and chronoamperometry were performed by using the Potentiostat/Galvanostat M 238 EG&G PAR (Princeton, NY) in conjunction with the M 270 (EG & G PAR) software. Unless otherwise stated, the reference electrode was an Ag/AgCl saturated KCl.

Procedure for Bi analysis in the pharmaceutical products

For the determination of bismuth in the pharmaceutical product, a tablet of the antiulcer De-Nol® was ground in a mortar and an accurate weighed amount (ca. 0.4 g) of powder was treated with concentrated HNO_3 and kept under stirring for about 30 min to allow complete dissolution of the bismuth salts; afterwards, the solution was brought to 50 ml. The appearance of the latter solution was slightly milky, due to the presence of suspended colloidal particles in the medium. The analysis of the bismuth content was made after transferring 25 μl of the latter solution (without any further treatment) to 25 ml of 0.5 M H_2SO_4 solution and running the UPD-SV procedure, as described below. The multiple standard addition was used for quantification.

Results and discussion

Diffusional characteristics of the Pt-MEs

Preliminarily, the diffusional characteristics of the Pt-MEs were investigated by CV in 1 mM Ru $(NH_3)_6^{3+}$+0.1 M KCl aqueous solution at 5 mV s^{-1}. The voltammograms obtained with all Pt-MEs provided sigmoidal waves (not shown), as expected for microelectrodes working under steady state conditions [23]. This indicated that the non-uniform current density distribution typical of a micro-disk was not affected by the platinum nanostructure. Therefore, as for other microelectrodes, the enhanced mass transport, also applying to the Pt-MEs, obviated for the need of hydrodynamic conditions during the pre-concentration step [3]. Thus, all UPD-SVs described in this work were performed under quiescent conditions.

Cyclic voltammetry at Pt-MEs in 0.5 M H_2SO_4 containing Bi^{3+} ions

Figure 1 shows typical cyclic voltammograms recorded with a Pt-ME (*RF*=140) in 0.5 M H_2SO_4 base electrolyte without

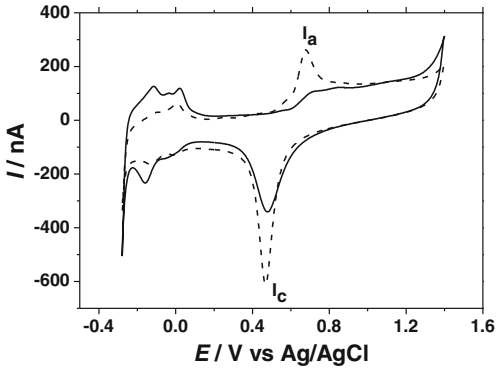

Fig. 1 Cyclic voltammograms recorded at a Pt-ME (*RF*=262) in 0.5 M H_2SO_4 without (—) and with 1 mM $Bi(NO_3)_3$ (---). Scan rate 100 mVs^{-1}

(solid line) and with 1 mM $Bi(NO_3)_3$ (dashed line) after cycling the potential several times over the range from −0.4 to 1.4 V. In the absence of Bi^{3+} ions, the voltammetric pattern is that expected for polycrystalline platinum and shows peaks due to hydrogen adsorption/desorption (from −0.3 to ~0.1 V), the double layer region (from ~0.1 to ~0.3 V) and platinum oxides formation and reduction (from ~0.3 to ~1.1 V) [24]. In the presence of bismuth ions, the hydrogen adsorption/desorption peaks are somewhat depressed, which is due to the fact that hydrogen does not adsorb on Bi(0) [25], while two new peaks I_a and I_c appear over the potential region where Pt oxide formation/reduction occurs. The latter two peaks are due to the oxidation/reduction of bismuth species adsorbed onto the Pt surface, which overlap with the platinum oxide processes [25–29]. The presence of peak I_c, during the cathodic scan, is due to the fact that, on platinum, bismuth is irreversibly deposited [25]. Oxidised bismuth species, comprising various oxides/hydroxides, are formed during the anodic scan and then retained on to the Pt surface [28]. They can therefore be reduced during the cathodic scan. This is opposite to the UPD behaviour reported at mesoporous platinum electrodes for the metal ions Ag^+, Pb^{2+} and Cu^{2+}, for which only the anodic peak was shown to increase under experimental conditions similar to those employed here [13, 14]. The irreversible adsorption of bismuth species on to the platinum surface is an issue that needs to be considered for setting up a reliable procedure for the determination of bismuth by UPD-SV free from memory effects (vide infra).

UPD-SV of bismuth at Pt-MEs

Bismuth accumulation onto the electrode surface could also be achieved by under-potential deposition at a constant potential, i.e., over the double layer potential region from 0.1 to 0.2 V [22]. This procedure was therefore used throughout to investigate the effect of Bi^{3+} concentrations on the cyclic voltammograms. Figure 2a shows a series of

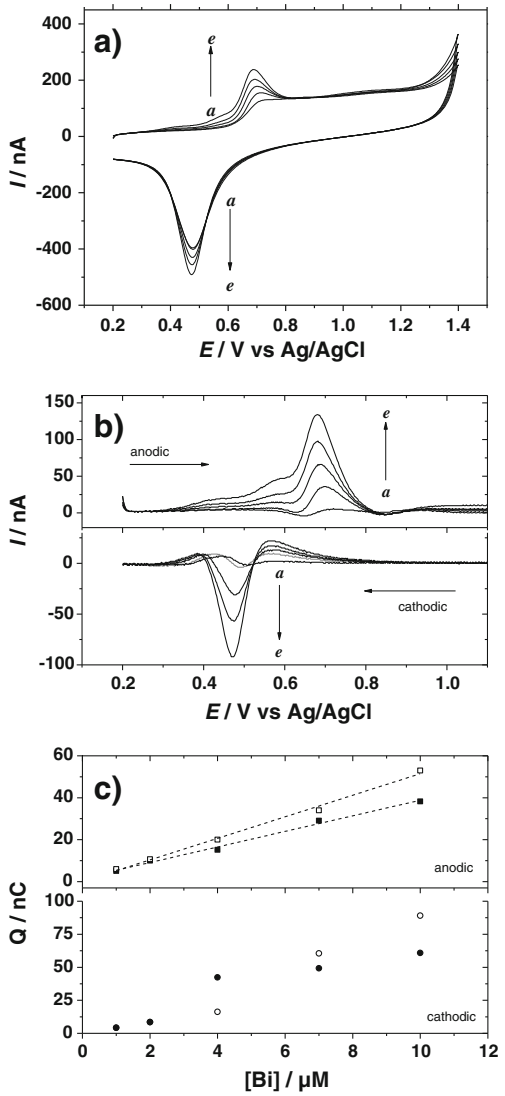

Fig. 2 **a** Cyclic voltammograms recorded after bismuth accumulation for 240 s at 0.2 V in 0. 5 M H_2SO_4 solution containing: *a* 1, *b* 2, *c* 4, *d* 7 and *e* 10 μM Bi^{3+}. **b** Corresponding anodic and cathodic peak subtracted by the blank recorded in 0. 5 M H_2SO_4. **c** Calibration plots of charge vs. bismuth concentration for the anodic peak at accumulation times of t=120 s (■) and t=240 s (□), and cathodic peak at t=120 s (●) and t=240 s (○)

CVs recorded over the potential range 0.2–1.4 V after performing the bismuth accumulation for 240 s at 0.2 V in a 0.5 M H_2SO_4 solution containing increasing amounts of Bi^{3+} in the range 1–10 μM. As is evident, both peaks I_a-I_c increase as the bismuth concentration increases, indicating an efficient accumulation of bismuth on the electrode surface. It must be remarked that over the above concentration levels, no sensible accumulation of bismuth could be achieved by carrying out a single CV with no pre-concentration at the UPD potential. These results therefore suggest that the I_a-I_c peak system can be used for the quantification of low Bi^{3+} concentrations, provided that a pre-concentration step is performed. Calibration graphs were constructed by using the charge involved in either the anodic (Q_a) or cathodic (Q_c) peaks, after subtracting the charge due to the platinum oxide formation and reduction, respectively. An example of such exercise is shown in Fig. 2b, while Fig. 2c shows typical calibration plots thus obtained using accumulation times of 120 and 240 s. Figure 2b highlights that the CVs, in the anodic scan display, along with the main peak I_a, two smaller peaks, the latter occurring at less positive potentials. This CV profile was already noticed in earlier works and was associated with the stepwise oxidation of bismuth ad-layers by dissociative adsorption of water [22, 28, 30]. As for the calibration plots shown in Fig. 2c, it is evident that only the anodic charge displays a satisfactory linear relationship with bismuth concentration regardless of the accumulation time employed. Moreover, both anodic and cathodic charges do not appear to correlate with the accumulation time. These results can be explained considering several factors affecting both the accumulation and stripping processes of bismuth, including surface kinetics, surface saturation, memory effects due to the irreversibly adsorbed bismuth, and, probably, the release of some amounts of bismuth during the anodic scan [20, 21, 28](see also below).

As regards to the Pt-ME surface coverage during the pre-concentration step, it conceivably occurs under mixed kinetic-diffusion control [13]. This is somewhat connected with the slower diffusion of the metal ions down the mesopores. However, for a given Pt-ME and deposition time, this effect should play a constant role and therefore should not affect the analytical performance of the Pt-ME. Problems related to the saturation of the Pt-ME's surface by bismuth could also be excluded. In fact, the highest charge involved in the calibration plots amounted to 149 μC cm^{-2}, which is about 33 % of 460 μC cm^{-2}, the latter being the charge needed to deposit a mono-layer of bismuth [26]. Thus, the release of bismuth from the Pt-MEs and memory effects, which are closely connected, probably play the main role in the ability to perform reliable analytical measurements of Bi^{3+} ions using Pt-MEs. These aspects were examined in detail and described below.

Stability of irreversibly deposited bismuth

The release of amounts of adsorbed bismuth from the electrode surface to the solution was already observed in earlier works. This phenomenon was found to depend on the upper anodic potential set in CV experiments [20, 21, 28]. In fact, it was shown that Bi-loaded Pt-MEs progressively released the adsorbed bismuth when the upper potential in CV experiments was set to values higher than 0.9 V vs. Ag/AgCl [20, 21, 28]. This circumstance was further investigated here using a Pt-ME (RF=260) fully loaded with

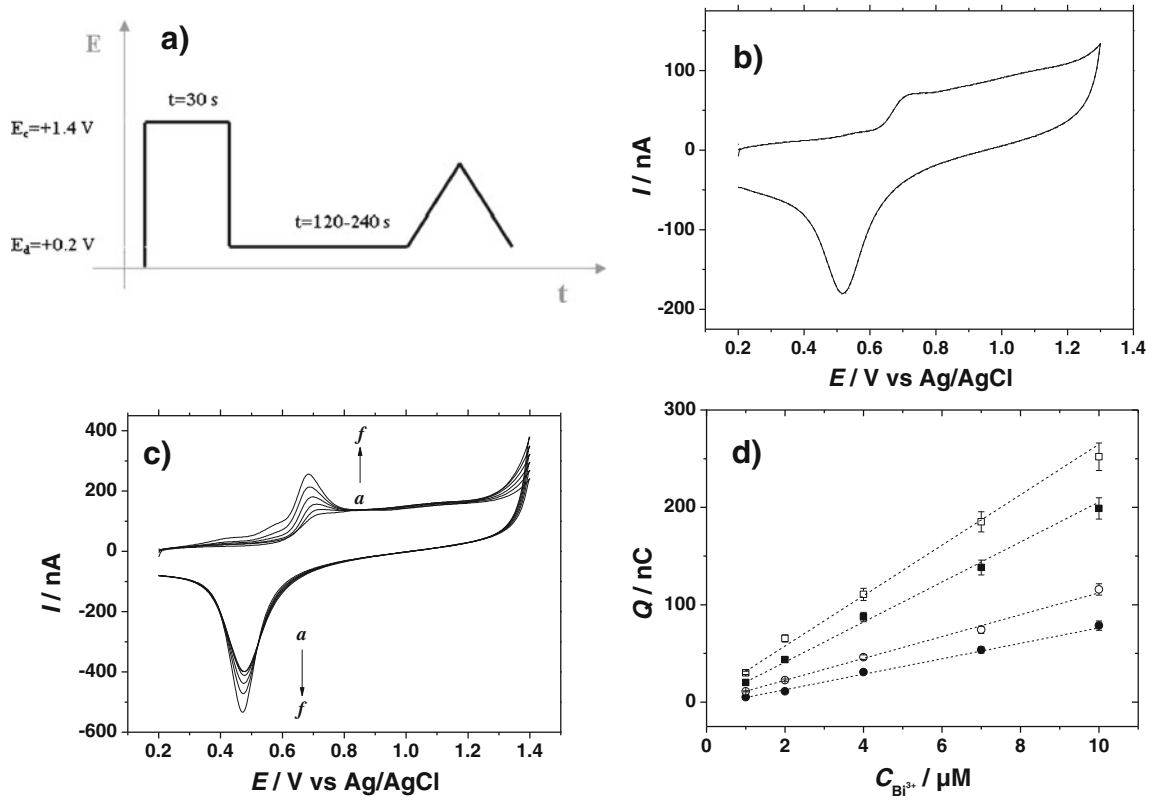

Fig. 3 **a** Applied waveform for bismuth determination. **b** Three subsequent UPD-SVs recorded in 0.5 M H_2SO_4+1 mM Bi^{3+}. **c** CVs recorded after bismuth accumulation for 240 s at+0.2 V in 0.5 M H_2SO_4 containing *a* 0, *b* 1, *c* 2, *d* 4, *e* 7 and *f* 10 μM Bi^{3+}. **d** Calibration plot of charge obtained from the anodic peaks at accumulation times of t=120 s (■) and t=240 s (□), and cathodic peaks at t=120 s (●) and t=240 s (○) vs. bismuth concentration

bismuth, transferred in 0.5 M H_2SO_4 solution free from Bi^{3+} ions and varying the anodic potential up to obtain the CV recorded with the pristine Pt-ME. It was verified that the Bi-loaded Pt-ME recovered its initial conditions after performing 15–20 CVs at 100 mV s^{-1} and setting the upper potential limit to 1.4 V. The latter result also indicated that no or negligible loss of *RF* during the above experiments occurred. A similar good recovering result was also obtained by applying to the Bi-loaded Pt-ME a constant potential equal to 1.4 V for a sufficient long time. The latter depended on the amount of bismuth initially adsorbed onto the electrode surface and on the *RF* of the Pt-ME. Based on these results, a procedure for reproducible and memory effect-free detection of bismuth was set as illustrated in the next section.

UPD-ASV procedure for Bi^{3+} detection at Pt-MEs

A suitable waveform that allowed the reproducible detection of Bi^{3+} at the Pt-MEs over the concentration range 1–10 μM is shown in Fig. 3a. It comprises a cleaning step performed at 1.4 V for 30 s; a deposition step carried out at 0.2 V for 120 or 240 s and a CV run from 0.2 to 1.4 V at 100 mV s^{-1}. The time employed in the cleaning step was optimised in a 0.5 M H_2SO_4 solution containing 10 μM Bi^{3+} ions (i.e., the largest Bi^{3+} concentration employed in the calibration plots, where memory effects could be more important). Under these conditions, reproducibility of the UPD-SV responses was within 4 % (three replicates), regardless of *RF* of the Pt-MEs. Figure 3b illustrates how well three subsequent UPD-SVs, taken with the same Pt-ME, overlap. This result indicates that

Table 1 Regression parameters of the calibration plots obtained from the UPD-SVs in 0.5 M H_2SO_4 solutions containing Bi^{3+} over the concentration range 1–10 μM, using different times (t) as indicated

	Anodic peak		Cathodic peak	
	t=120 s	t=240 s	t=120 s	t=240 s
R[a]	0.997	0.997	0.998	0.999
Slope (nC μM^{-1})	19.53±0.53	24.31±0.70	8.23±0.19	11.37±0.43
LOD (μM)	0.71	0.52	0.83	0.62

[a]Regression coefficient

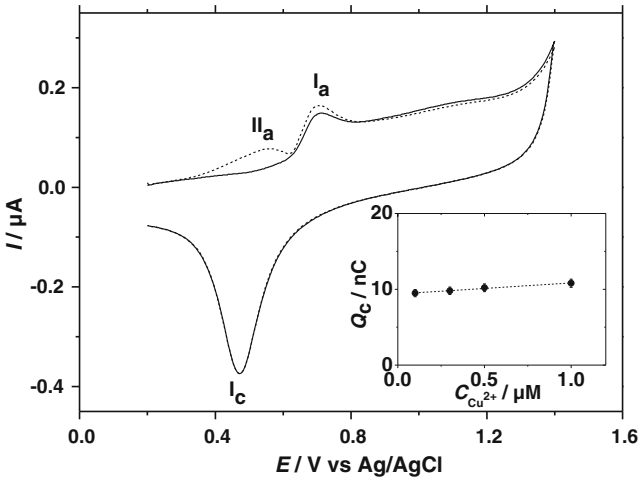

Fig. 4 CVs recorded in 0.5 M H_2SO_4+1 μM Bi^{3+} without (—) and with (---) 2 μM Cu^{2+}. *Inset* charge involved in the cathodic peak vs. Cu^{2+} concentration

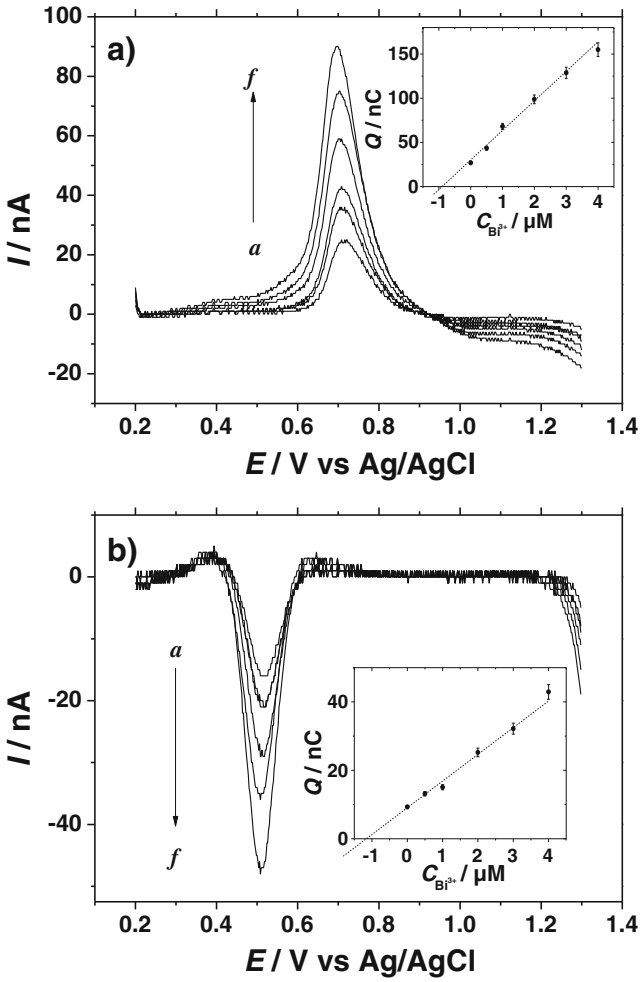

Fig. 5 Anodic (**a**) and cathodic (**b**) peaks subtracted by blank in De-Nol determination. Bismuth addition from *a* 0, *b* 0.5, *c* 1, *d* 2, *e* 3 and *f* 4 mM. *Inset* corresponding calibration plots

Table 2 Regression parameters of the multiple standard addition plots used for the determination of bismuth in a De-Nol® tablet. Dynamic range 1–4 μM

	Anodic peak (t=240 s)	Cathodic peak (t=240 s)
Slope (nC μM^{-1})	32.15±1.36	8.34±0.38
Intercept (nC)	30.54±2.06	8.21±0.46
R	0.997	0.998

t Deposition time at 0.2 V as indicated

the application of the waveform of Fig. 3a allows minimising memory effects, which could arise from the irreversibly adsorbed bismuth onto the electrode surface. Figure 3c shows typical UPD-SVs recorded with a Pt-ME (*RF*=260) over the Bi^{3+} concentration range 1–10 μM, following the application of the latter waveform; Fig. 3d displays relevant calibration plots. As is evident, in these conditions, the plots are linear for both anodic and cathodic charges with slopes (i.e., sensitivity) and correlation coefficients shown in Table 1. This table also includes lower detection limits obtained on the basis of the bismuth UPD-SV charges three times larger than the standard deviation of the blank, which is due to the charge associated to the oxide formation/reduction.

Since repetition of the UPD/stripping steps during measurements could damage somewhat the mesoporous structure, long-term stability of the Pt-MEs was also ascertained. This test was performed in aliquots of a 0.5 M H_2SO_4 solution containing 5 μM Bi^{3+} ions, using the same Pt-ME for 4 weeks, and evaluating the Bi^{3+} content with the standard addition approach (about 20 UPD-SV measurements). It was found that the investigated electrode system kept, essentially, its initial performance. However, the real surface area (i.e., *RF*) decreased to some extent (~5–7 %/week), probably due to the loss of the architecture of the mesoporous nanostructure.

All the above results, overall, indicate that the use of the UPD-SV procedure proposed here offers a reliable method for the detection of Bi^{3+} in aqueous media.

Interference

ASV of bismuth based on bulk metal deposit at solid electrodes is normally complicated by interference due to copper,

Table 3 Amounts of bismuth, expressed as Bi_2O_3, determined in a De-Nol® tablet by UPD-SV and titration with EDTA

Method	Bi_2O_3 (mg/tablet)
Anodic peak	122.6±4.9
Cathodic peak	118.2±4.3
EDTA	123.1±4.2
From the provider	120

whose stripping peak overlaps to a large extent with that of bismuth [31, 32]. The effect of Cu^{2+} concentration on the UPD-SV responses of bismuth, following the application of the waveform of Fig. 3a, was investigated in a 0.5 M H_2SO_4 solution containing 1 μM Bi^{3+} to which increasing amounts of Cu^{2+} (in the range 1–10 μM) were added. Figure 4 shows typical UPD-SVs obtained by using a Pt-ME (*RF*=260) in a sulphuric acid solution containing 1 μM Bi^{3+} (full line) and 1 μM Bi^{3+}+2 μM Cu^{2+} (dashed line). As is evident, in the presence of copper ions, the peak II_a, cathodic to I_a, was recorded. Peak II_a is located at potentials similar to those reported in the literature and attributed to copper underpotential deposition (Cu-UPD) at polycrystalline platinum electrodes [33–35]. Although the Cu-UPD peak is well distinguishable from the main peak I_a, it interfered somewhat with the Bi detection, when the Q_a vs. Bi^{3+} concentration plot was employed for quantification. However, using the Q_c vs. Bi^{3+} concentration plot, interference was minimal. As an example, inset in Fig. 4 shows how the Q_c of peak I_c varies with Cu^{2+} concentration. This result is consistent with the circumstance that copper does not provide irreversibly adsorbed deposits, and therefore any Cu-UPD, eventually accumulated together with Bi-UPD, is released in the solution during the anodic scan or in the cleaning step.

The effect of oxygen on the UPD-SV responses of the Pt-MEs was also checked by performing a series of measurements in either air- or nitrogen-saturated solutions. It was found that the UPD-SV responses recorded in the two different conditions did not differ more than 4 % (rsd), thus indicating no or negligible interference from oxygen present in the solution. This result is congruent with the circumstance that the UPD-SV procedure involves only a potential region sufficiently anodic the oxygen reduction process (i.e., about 0.23 V vs. Ag/AgCl) [18].

Determination of bismuth in antiulcer De-Nol® tablets

The above proposed procedure was applied to the analysis of a tablet of the commercial pharmaceutical product De-Nol®, used for curing ulcers. According to the providers, the tablet examined contained tripotassium dicitratobismuthate at a concentration corresponding to 120 mg of Bi_2O_3 per tablet. The determination of the analyte was performed after dissolution of the tablet as described in the "Experimental" section. Figure 5 shows typical UPD-SV responses obtained after subtracting the background charge due to platinum oxide formation/reduction and the plots of charges against the Bi^{3+} concentration added to the sample. Each datum of the calibration plots is the average value of four replicates. Table 2 shows the parameters of the calibration plots obtained from the linear regression analysis of the experimental points. The accuracy of the developed method was checked by comparison of the results obtained by UPD-SV to that found using the method based on EDTA titration with xylenol orange as indicator. Data obtained with the different methods, expressed as Bi_2O_3 are shown in Table 3. As is evident, data obtained by UPD-SV compare well with either the value indicated by the provider or that found by the classical EDTA titration.

Conclusions

In this paper, an analytical methodology for the detection of Bi^{3+} at mesoporous platinum microelectrodes has been assessed. It is based on the UPD-SV of bismuth irreversibly adsorbed onto the surface of the nanostructure. The UPD-SV procedure employed here allows overcoming interference due to copper and oxygen, which is normally observed when quantification of bismuth is performed by ASV at solid electrodes involving bulk metal deposits. The method developed here has been applied to a pharmaceutical preparation with minimal pre-treatments of the sample. Because metal UPD involves mainly the internal pores of the mesoporous structure, interference arising from particulate matter suspended in the sample is minimal. The procedure proposed here is simple and faster than other instrumental analytical methods normally utilised for bismuth detection, such as spectrophotometric and colorimetric methods [36].

Acknowledgments Financial support of the Ministry of University and Scientific Research (MIUR) (PRIN-2010AXENJ8) is gratefully acknowledged.

References

1. Brown RJC, Milton MJT (2005) Trends Anal Chem 24:266–274
2. Wang J (1985) Stripping analysis: principles, instrumentation and applications. VCH, Deerfield Beach
3. Daniele S, Baldo MA, Bragato C (2008) Curr Anal Chem 4:215–228
4. Švancara I, Prior C, Hočevar SB, Wang J (2010) Electroanalysis 22:1405–1420
5. Brainina K, Neyman E (1993) Electroanalytical stripping methods. Wiley, New York
6. Baldo MA, Daniele S, Mazzocchin GA (1998) Electroanalysis 10:410–416
7. Kokkinos C, Economou A (2008) Curr Anal Chem 4:183–190
8. Hocevar SB, Švancara I, Ogorevc B, Vytřas K (2007) Anal Chem 79:8639–8643
9. Herzog G, Arrigan DWM (2005) Trends Anal Chem 24:208–217
10. Herrero E, Buller LJ, Abruna HD (2001) Chem Rev 101:1897–1930
11. Kolb DM (1978) In: Gerischer H, Thomas CW (eds) Advances in electrochemistry and electrochemical engineering, vol 11. Wiley, New York, p 125
12. Aramata A (1997) In: Bockis JOM, White RE, Conway BE (eds) Modern aspects of electrochemistry, vol 31. Plenum Press, New York, p 181

13. Lozano Sanchez P, Elliott JM (2005) Analyst 130:715–720
14. Lozano Sanchez P, Elliott JM (2008) Analyst 133:256–262
15. Attard GS, Bartlett PN, Coleman NRB, Ellliott JM, Owen JR, Wang JH (1997) Science 278:838–840
16. Salvador JA, Figueiredo SA, Pinto RM, Silvestre SM (2012) Future Med Chem 4:1495–1523
17. Elliott JM, Birkin PR, Bartlett PN, Attard GS (1999) Langmuir 15:7411–7415
18. Birkin P, Elliot JM, Watson YE (2000) Chem Commun 17:1693–1694
19. Evans SAG, Elliot JM, Andrews LM, Bartlett PN, Doyle PJ, Denuault G (2002) Anal Chem 74:1322–1326
20. Daniele S, Battistel D, Bergamin S, Bragato C (2010) Electroanalysis 22:1511–1518
21. Daniele S, Battistel D, Bragato C (2012) Electroanalysis 24:759–766
22. Daniele S, Bergamin S (2007) Electrochem Commun 9:1388–1393
23. Bard AJ, Faulkner LR (2001) Electrochemical methods. Wiley, New York
24. Noel M, Vasu KI (1990) Cyclic voltammetry and the frontiers of electrochemistry. Aspect Publications Ltd, London, p 347
25. Clavilier J, Feliu JM, Aldaz A (1988) J Electroanal Chem 243:419–433
26. Cadle SH, Bruckenstein S (1972) Anal Chem 44:1993–2001
27. Kang S, Lee J, Lee JK, Chung SY, Tak Y (2006) J Phys Chem B 110:7270–7274
28. Uhm S, Yun Y, Tak Y, Lee J (2005) Electrochem Commun 7:1375–1379
29. Tripković AV, Popovic KD, Stevanovic RM, Socha R, Kowal A (2006) Electrochem Commun 8:1492–1498
30. Yang M (2013) J Power Sources 229:42–47
31. Wang J, Lu J, Kirgöz UA, Hocevar SB, Ogorevc B (2001) Anal Chim Acta 434:29–34
32. Baldo MA, Daniele S (2004) Anal Lett 37:995–1011
33. Machado SAS, Tanaka AA, Gonzalez ER (1991) Electrochim Acta 36:1325–1331
34. Mascaro LH, Machado SAS, Avaca L (1997) J Chem Soc Faraday Trans 93:2577–2582
35. Miwa DW, Santos MC, Machado SAS (2006) J Braz Chem Soc 17:1339–1346
36. Burguera M, Burguera JL, Rondon C, Garcia MI, de Pena YP, Villasmil LM (2001) J Anal At Spectrom 16:1190–1195